

Geophysical Research Letters

RESEARCH LETTER

10.1029/2020GL087860

Key Points:

- We show evidence for nocturnal production of organic nitrates similar in magnitude to daytime photochemical production
- Significant nocturnal production of organic nitrates observed from three aircraft campaigns in distinct environments
- Nighttime production of organic nitrates impacts our understanding of the nighttime lifetime and fate of NO_x

Supporting Information:

- Supporting Information S1

Correspondence to:

R. C. Cohen,
 rccohen@berkeley.edu

Citation:

Kenagy, H. S., Sparks, T. L., Wooldridge, P. J., Weinheimer, A. J., Ryerson, T. B., Blake, D. R., et al. (2020). Evidence of nighttime production of organic nitrates during SEAC⁴RS, FRAPPÉ, and KORUS-AQ. *Geophysical Research Letters*, 47, e2020GL087860. <https://doi.org/10.1029/2020GL087860>

Received 6 MAR 2020

Accepted 16 MAY 2020

Accepted article online 11 MAR 2020

Evidence of Nighttime Production of Organic Nitrates During SEAC⁴RS, FRAPPÉ, and KORUS-AQ

Hannah S. Kenagy¹ , Tamara L. Sparks¹ , Paul J. Wooldridge¹ , Andrew J. Weinheimer² , Thomas B. Ryerson³ , Donald R. Blake⁴ , Rebecca S. Hornbrook² , Eric C. Apel² , and Ronald C. Cohen^{1,5} 

¹Department of Chemistry, University of California, Berkeley, CA, USA, ²Atmospheric Chemistry Observations & Modeling Laboratory, National Center for Atmospheric Research, Boulder, CO, USA, ³Chemical Sciences Division, NOAA Earth System Research Laboratory, Boulder, CO, USA, ⁴Department of Chemistry, University of California, Irvine, CA, USA, ⁵Department of Earth and Planetary Science, University of California, Berkeley, CA, USA

Abstract Organic nitrates (RONO_2) are an important NO_x sink. In warm, rural environments dominated by biogenic emissions, nocturnal NO_3 -initiated production of RONO_2 is competitive with daytime OH-initiated RONO_2 production. However, in urban areas, OH-initiated production of RONO_2 has been assumed dominant and NO_3 -initiated production considered negligible. We show evidence for nighttime RONO_2 production similar in magnitude to daytime production during three aircraft campaigns in chemically distinct summertime environments: Studies of Emissions and Atmospheric Composition, Clouds, and Climate Coupling by Regional Surveys (SEAC⁴RS) in the rural Southeastern United States, Front Range Air Pollution and Photochemistry Experiment (FRAPPÉ) in the Colorado Front Range, and Korea-United States Air Quality Study (KORUS-AQ) around the megacity of Seoul. During each campaign, morning observations show RONO_2 enhancements at constant, near-background O_x ($\equiv \text{O}_3 + \text{NO}_2$) concentrations, indicating that the RONO_2 are from a non-photochemical source, whereas afternoon observations show a strong correlation between RONO_2 and O_x resulting from photochemical production. We show that there are sufficient precursors for nighttime RONO_2 formation during all three campaigns. This evidence impacts our understanding of nighttime NO_x chemistry.

Plain Language Summary Nitrogen oxides are pollutants emitted during combustion which are involved in ozone and secondary aerosol production. One way in which nitrogen oxides are removed from the atmosphere is via chemistry that converts them to organic nitrates. This conversion of nitrogen oxides to organic nitrates has been thought to occur primarily during the day when the chemistry is driven by sunlight. Here we show evidence that nighttime processes generate similar quantities of organic nitrates to those produced by sunlight-driven processes.

1. Introduction

Nitrogen oxides ($\text{NO}_x \equiv \text{NO} + \text{NO}_2$) are important tropospheric oxidants that contribute to ozone (O_3) formation, secondary aerosol production, and nitrogen deposition to ecosystems. Alkyl and multifunctional organic nitrates (RONO_2) are an oxidative sink of NO_x . Previous studies have shown that RONO_2 production is a significant NO_x loss pathway (Day et al., 2003), especially as urban NO_x concentrations decrease (Perring et al., 2013; Romer Present et al., 2020). Organic nitrates can be generated through both daytime photochemical oxidation pathways initiated by OH and nighttime oxidation pathways initiated by NO_3 .

During the day, RONO_2 is produced photochemically as a radical termination step in a series of reactions between oxidized volatile organic compounds (VOCs) and NO_x (shown in Figure 1). VOCs are oxidized by OH to form organic peroxy radicals, RO_2 (R1). Reaction between NO and organic peroxy radicals can result in formation of an organic nitrate (R2, minor pathway, branching ratio α). The major pathway for the reaction between RO_2 and NO (R3), however, continues radical propagation to form two ozone molecules (R4, R5, R6). Consequently, this daytime chemistry produces both O_x ($\equiv \text{O}_3 + \text{NO}_2$) and RONO_2 so, if photochemistry is dominant, we expect a correlation between O_x and RONO_2 . Typically, chain lengths are such that we expect 6–20 O_x for each RONO_2 (Perring et al., 2013).

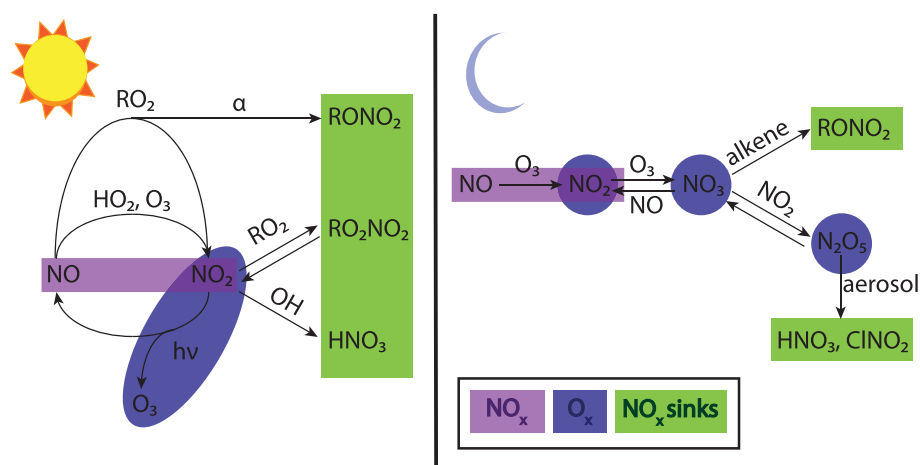
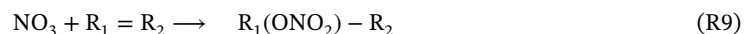


Figure 1. Schematic of daytime (left) and nighttime (right) NO_x chemistry.



At night, RONO_2 is produced from alkenes via addition of NO_3 to a double bond (R9), as shown in Figure 1. NO_3 is formed from reaction between NO_2 and O_3 (R8). During the day, NO_3 is lost quickly via reaction with NO or via photolysis. In the nocturnal residual layer removed from fresh NO emissions, NO_3 concentrations can build up and react with alkenes. Two O_3 molecules are consumed in the production of NO_3 (R7 followed by R8), meaning that nighttime RONO_2 formation is a net sink of O_x . Consequently, we do not expect a positive correlation between RONO_2 and O_x if NO_3 is the dominant oxidant, and we might even expect a weak negative correlation.



The fate of NO_x at night is controlled by the balance of two NO_3 reaction pathways. First, NO_x can be lost via NO_3 reaction with alkenes, as described above. Second, NO_3 can be lost at night via reaction with NO_2 to form N_2O_5 in thermal equilibrium, followed by aerosol uptake and heterogeneous hydrolysis to produce HNO_3 and ClNO_2 . In certain environments, NO_3 may also react with species such as dimethyl sulfide, aldehydes, and peroxy radicals. The competition between these reaction pathways is controlled by both the relative availability of alkenes and by the fate of N_2O_5 . Nighttime RONO_2 production increases in environments with high biogenic alkene emissions (isoprene, monoterpenes) and in environments with high anthropogenic alkene emissions, particularly where either of these two emission sources is sustained overnight. The N_2O_5 loss pathway becomes less competitive with RONO_2 formation in environments with

low aerosol surface area and small heterogeneous uptake coefficients for N_2O_5 ($\gamma(\text{N}_2\text{O}_5)$), as these decrease the rate of heterogeneous hydrolysis of N_2O_5 . Additionally, higher temperatures shift the N_2O_5 equilibrium towards dissociation, making N_2O_5 formation less favorable, while also increasing the rate of bimolecular NO_3 reactions with alkenes. Thus, nighttime RONO_2 formation is most favorable in environments with high alkene emissions, low aerosol surface area, small $\gamma(\text{N}_2\text{O}_5)$, and high temperature.

There is reason to suspect that RONO_2 production from nighttime NO_3 oxidation of VOCs could be competitive with RONO_2 production from photochemical OH oxidation. Because it is removed from fresh overnight NO emissions, a chemically active residual layer characteristic of many nighttime environments can contain elevated NO_3 concentrations as well as VOC emissions from late in the day. Moreover, RONO_2 yields from NO_3 -initiated oxidation (20–80%) are far larger than RONO_2 yields from OH-initiated oxidation of VOCs (0.1–35%) (Perring et al., 2013 and references within). Even if NO_3 oxidation represents a smaller fraction of total VOC oxidation than OH oxidation, the larger RONO_2 yields could make RONO_2 production from NO_3 oxidation competitive with RONO_2 production from OH oxidation.

A number of recent studies have shown that NO_3 oxidation can be a significant source of RONO_2 in regions dominated by biogenic VOC emissions. In forested regions of Colorado, Finland, and Germany, nighttime concentrations of RONO_2 were found to be comparable with daytime RONO_2 concentrations (Fry et al., 2013; Liebmann et al., 2019; Sobanski et al., 2017). Other studies have found NO_3 -initiated formation of isoprene nitrates to be competitive with OH-initiated formation of isoprene nitrates in the Southeastern United States (Starn et al., 1998; Xiong et al., 2015), in an observationally constrained model of the eastern United States (Horowitz et al., 2007), and in a global model (von Kuhlmann et al., 2004).

Moreover, NO_3 oxidation has been shown to be a significant source of organic aerosol in the Central Valley of California (Rollins et al., 2012), the Southeastern United States (Ayres et al., 2015; Fisher et al., 2016; Lee et al., 2016; Pye et al., 2015; Xu, Guo et al. 2015; Xu, Suresh et al. 2015), in a forested region of Colorado (Fry et al., 2013), in rural Southwestern Germany (Huang et al., 2019), throughout Europe (Kiendler-Scharr et al., 2016), and in the Alberta oil sands (Lee et al., 2019).

Though NO_3 chemistry has been shown to be an important source of RONO_2 and secondary organic aerosol in rural regions dominated by biogenic emissions, nocturnal NO_3 -initiated RONO_2 formation has often been considered negligible in comparison with daytime OH-initiated production of RONO_2 in urban environments. In this study, we present evidence for significant nighttime RONO_2 production using measurements of O_x and RONO_2 from three aircraft-based field campaigns in distinct summertime environments. First, we show evidence for significant nighttime RONO_2 production in the rural southeastern United States during Studies of Emissions and Atmospheric Composition, Clouds, and Climate Coupling by Regional Surveys (SEAC^4RS), an area with high biogenic emissions. Second, we show similarly high nighttime RONO_2 production in two urban areas: in the Colorado Front Range during Front Range Air Pollution and Photochemistry Experiment (FRAPPÉ), which is affected by both high urban and oil/gas emissions, as well as in and around the megacity of Seoul during Korea-United States Air Quality Study (KORUS-AQ). In each location, we show that the expected linear relationship between O_x and RONO_2 is observed during the afternoon. However, during the morning hours, the relationship between O_x and RONO_2 shows evidence of nighttime RONO_2 production. We support this conclusion further by assessing precursor availability for nighttime RONO_2 production.

2. Measurements

2.1. SEAC^4RS , FRAPPÉ, and KORUS-AQ Aircraft Campaigns

The SEAC^4RS campaign took place during August and September 2013 in the Southeastern and Western United States (Toon et al., 2016). This analysis uses observations from the NASA DC-8 aircraft which flew 19 primarily daytime research flights out of Ellington Field, near Houston, TX.

The FRAPPÉ campaign took place during July and August 2014 in the Northern Front Range Metropolitan Area (NFRMA) of Colorado (Flocke et al., 2020). This analysis uses observations from the NSF/NCAR C-130 aircraft which flew 15 daytime research flights out of the Rocky Mountain Metropolitan Airport in Jefferson County, CO.

The KORUS-AQ campaign took place during May and June 2016 over South Korea and the Yellow Sea (Nault et al., 2018). This analysis uses observations from the NASA DC-8 aircraft which flew 20 daytime research flights out of Pyeongtaek, South Korea (≈ 60 km south of Seoul).

2.2. Instrumentation

During all three campaigns, measurements of NO_2 and total RONO_2 (including both gas-phase and particle-phase RONO_2) were made by the UC Berkeley thermal dissociation laser-induced fluorescence (TD-LIF) instrument (Day et al., 2002; Wooldridge et al., 2010). Briefly, one channel of the instrument measures NO_2 by laser-induced fluorescence. Two other channels first flow air through a heated quartz oven. One channel is set at 180°C , the temperature at which peroxy nitrates (RO_2NO_2) dissociate into RO_2 and NO_2 . The second is set at 360°C , the temperature at which RONO_2 dissociate into $\text{RO} + \text{NO}_2$. The difference in NO_2 detected in adjacent channels gives the mixing ratio for each class of compounds: the RO_2NO_2 mixing ratio is the difference between the 180°C channel and the unheated channel, and the RONO_2 mixing ratio is the difference between the 360°C channel and the 180°C channel.

O_3 and NO were measured by chemiluminescence. During SEAC⁴RS, O_3 and NO were measured by the NOAA NO_yO_3 instrument (Ryerson et al., 1999, 2000). During FRAPPÉ and KORUS-AQ, O_3 and NO were measured by the NCAR chemiluminescence instrument (Ridley et al., 1994; Weinheimer et al., 1994).

Alkenes were measured by whole air sampling (WAS) (Colman et al., 2001; Simpson et al., 2011) and trace organic gas analyzer (TOGA) (Apel et al., 2015). For SEAC⁴RS and KORUS-AQ, we use WAS measurements of propene, butenes, isoprene, α -pinene, and β -pinene. During FRAPPÉ, we use WAS measurements of propene, isoprene, α -pinene, and β -pinene and TOGA measurements of butenes and limonene.

Instrument details, including accuracy and sampling interval, can be found in Table S1 of the Supporting Information. We use 1-min averaged data, and we consider only boundary layer data (below 1 km during SEAC⁴RS and KORUS-AQ and below 2 km during FRAPPÉ).

3. Observations/Results

3.1. O_x versus RONO_2

The relationship between O_x and RONO_2 during each campaign is shown in Figure 2 (plots of the relationship between O_x and RONO_2 during each flight within each campaign are shown in Figures S1–S6). During all three campaigns, during the afternoon hours (13:00–19:00 local time) when photochemistry is most active, there is a positive, linear relationship between O_x and RONO_2 , indicating that photochemical production of both O_x and RONO_2 is occurring. The slope of the relationship between O_x and RONO_2 mixing ratios is indicative of the branching ratio between O_x and RONO_2 production. From Figure 2, during SEAC⁴RS, 29 O_x are produced for each RONO_2 . Chain lengths are shorter during FRAPPÉ, where 13 O_x are produced for each RONO_2 , and longer during KORUS-AQ, where 43 O_x are produced for each RONO_2 .

During the morning hours (before 11:00 local time) before peak photochemistry occurs, however, the relationship between O_x mixing ratios and RONO_2 mixing ratios has a flat (zero) slope. At a relatively constant observed O_x mixing ratio, a wide range of RONO_2 mixing ratios was observed. This indicates that O_x and RONO_2 are not produced from the same pathway. Instead, the high levels of RONO_2 at relatively low levels of O_x suggest that much of the observed RONO_2 was produced via a non-photochemical pathway that produces RONO_2 without generating O_x . Since this trend is only observed in the morning, and not in the afternoon, it is indicative of a large source of RONO_2 produced from NO_3 oxidation overnight.

We also explored the effects of O_3 deposition and nighttime dynamics, but neither could sufficiently explain the observed trend. Estimating an approximate O_3 deposition velocity of 0.5 cm s^{-1} (e.g., Colbeck & Harrison, 1985; Lenschow et al., 1981) and boundary layer height of 1 km, the lifetime of O_3 to deposition is 56 h, far longer than the chemical timescales relevant to this analysis. Entrainment of air from aloft could also affect observed morning mixing ratios, but would have the same relative effect on both O_3 and RONO_2 . Consequently, neither O_3 deposition nor entrainment can explain the lack of correlation between O_x and RONO_2 in the morning; the observed effect can only be explained by significant nocturnal production of RONO_2 .

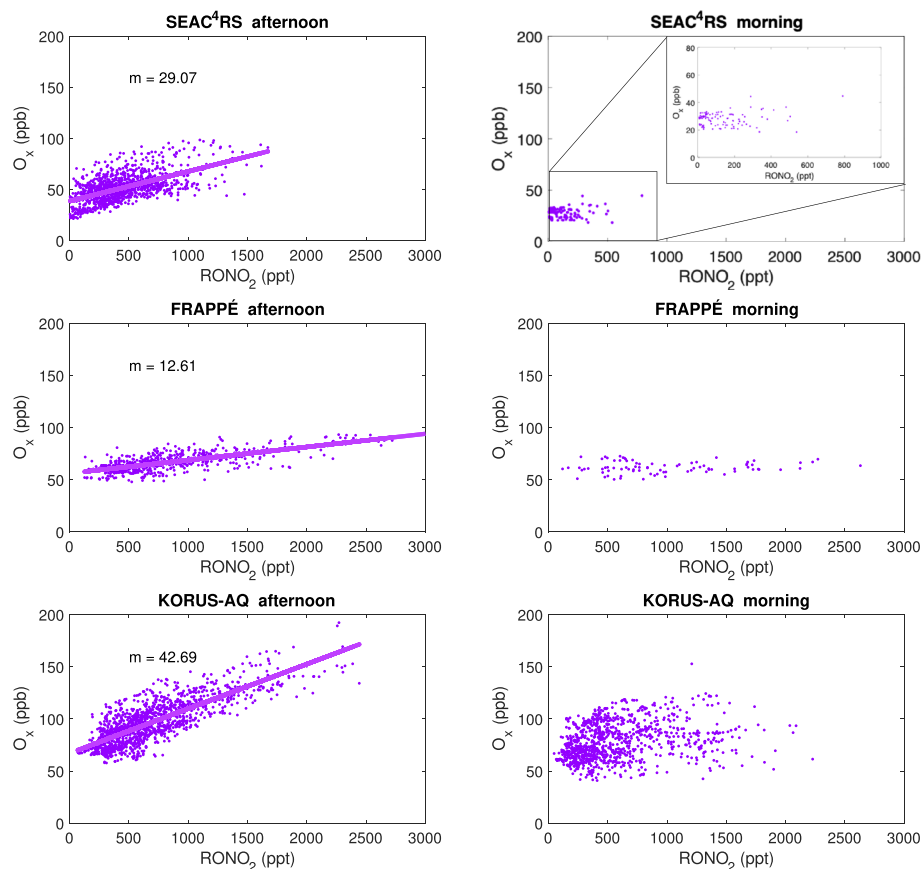


Figure 2. Plots of O_x vs. $RONO_2$ during SEAC⁴RS, FRAPPÉ, and KORUS-AQ during afternoon (left, 13:00–19:00 local time) and morning (right, before 11:00 local time). Only data in the boundary layer (<1 km for SEAC⁴RS and KORUS-AQ, <2 km for FRAPPÉ) are included. York linear fits (with slopes labeled as m) to the afternoon data are shown.

3.2. Precursors for Nighttime $RONO_2$ Production

As additional evidence for nighttime $RONO_2$ production, we assess the availability of precursors to $RONO_2$ production, namely NO_3 and alkenes. We report average morning (before 11:00 local time) mixing ratios of $RONO_2$, alkenes, and NO_x in Table 1. The abundance of NO_x and alkenes observed in the morning indicates that these precursors are not depleted by overnight chemistry; rather, the non-zero concentrations of precursors in the morning suggests that NO_3 -initiated $RONO_2$ production chemistry is sustained overnight and occurs until daybreak.

During SEAC⁴RS, there were insufficient morning alkene measurements to report meaningful averages. However, Edwards et al. (2017) report airborne measurements which show that the nocturnal residual layer in the Southeastern United States is rich in isoprene, evidence that there is an abundance of alkenes available overnight to form alkyl nitrates.

Moreover, we use the observed morning mixing ratios of NO_x , O_3 , and alkenes to calculate lower bounds on the integrated overnight production of NO_3 (Equation 1), the instantaneous production rate of $RONO_2$ (Equation 2), and the instantaneous production rate of alkenes + O_3 (Equation 3).

$$\int P(NO_3) = NO_{x,initial} (1 - \exp(-t \times k_{NO_2+O_3} \times [O_3])) \quad (1)$$

$$P(RONO_2) = \sum_i \alpha_i \times k_{NO_3+alkene_i} \times [alkene_i] \times [NO_3] \quad (2)$$

$$Rate(O_3 + alkene) = \sum_i k_{O_3+alkene_i} \times [alkene_i] \times [O_3] \quad (3)$$

Table 1

Table of the Average RONO₂, Alkene, and NO_x Concentrations in the Morning (Before 11:00 Local Time), Integrated Overnight Production of NO₃, Instantaneous Production Rate of RONO₂, and Instantaneous Reaction Rate of Alkenes with O₃

	SEAC ⁴ RS	FRAPPÉ	KORUS-AQ
RONO ₂ (ppb)	0.12	0.98	0.56
propene (ppt)	N/A	98	129
butene (ppt)	N/A	39	60
isoprene (ppt)	N/A	109	54
α-pinene (ppt)	N/A	11	15
β-pinene (ppt)	N/A	9.0	11
limonene (ppt)	N/A	4.8	N/A
NO _x (ppb)	0.43	8.1	4.4
∫ P(NO ₃) (ppb) ^a	0.23	5.2	2.9
P(RONO ₂) (ppb/h) ^{a,b,c}	N/A	2.3	1.3
alkene + O ₃ rate (ppb/h) ^{a,b}	N/A	0.021	0.108

Note. There are insufficient morning SEAC⁴RS measurements due to data sparsity to report meaningful morning average alkene mixing ratios. ^aCalculated from morning (before 11:00 local time) precursor observations and can therefore be considered a lower bound. ^bRate constants from MCM v3.3.1 are used. ^cNitrate yields used are from Perring et al. (2013) and references therein.

As shown in Table 1, the integrated production of NO₃ exceeds the observed morning mixing ratios of RONO₂, and the production rates of RONO₂ calculated from morning observations are more than sufficiently fast to account for the morning observations of RONO₂. Lastly, the rate of VOC (ethyne, ethene, propene, MACR, MVK, isoprene, butene, α-pinene, β-pinene, and limonene) oxidation by O₃ is at least an order of magnitude smaller than the production rate of RONO₂, indicating that NO₃ is the dominant nocturnal alkene oxidant in these environments.

4. Discussion and Conclusion

We show evidence of significant nighttime RONO₂ production during three aircraft campaigns in three distinct locations: the rural southeastern United States dominated by biogenic emissions (SEAC⁴RS), the Colorado Front Range dominated by a combination of urban and oil/gas emissions (FRAPPÉ), and the megacity of Seoul dominated by urban emissions (KORUS-AQ). Though, in urban areas, nighttime production of RONO₂ has often been considered negligible in comparison with daytime production, we show evidence for nighttime RONO₂ production that results in morning RONO₂ mixing ratios of similar magnitude to afternoon observations of RONO₂ in all three of these distinct environments.

Rapid nighttime RONO₂ production impacts our understanding of the lifetime and fate of NO_x at night. Evidence for nighttime RONO₂ production indicates that HNO₃ and ClNO₂ produced via heterogeneous hydrolysis of N₂O₅ are not necessarily the dominant nighttime sinks of NO_x, consistent with other aircraft-based nighttime urban NO₃ budgets (Brown et al., 2011). In environments with low aerosol loading, high temperatures, and an abundance of alkenes, RONO₂ production can be the dominant nighttime NO_x sink. Significant nocturnal NO₃-initiated RONO₂ production in urban areas also has implications for substantial overnight secondary organic aerosol production in and around cities.

We explore the effects of temperature, alkenes, and aerosol surface area on the fraction of NO_x lost as RONO₂ (defined as $\frac{P(\text{RONO}_2)}{P(\text{RONO}_2) + P(\text{HNO}_3)}$) at night in Figure 3, assuming an initial NO₂ concentration, constant O₃, pressure, and $\gamma(\text{N}_2\text{O}_5)$, and NO₃ and N₂O₅ in steady state (see Appendix A). Under these model conditions, the temperature, pressure, alkenes, NO₂, O₃, and aerosol surface area measured in the evening (after 16:30 local time) during FRAPPÉ and SEAC⁴RS indicate that RONO₂ is the dominant sink of NO_x at night and during KORUS-AQ indicate that overnight NO_x loss is evenly split between N₂O₅ loss and RONO₂ production. This is consistent with a tower-based measurement in Seoul in 2015 which showed rapid NO₃-BVOC chemistry (Brown et al., 2017). For contrast, during the WINTER campaign (aircraft campaign over NE US, February to March 2015), low temperatures and low alkene concentrations lead to NO_x loss at night dominated by

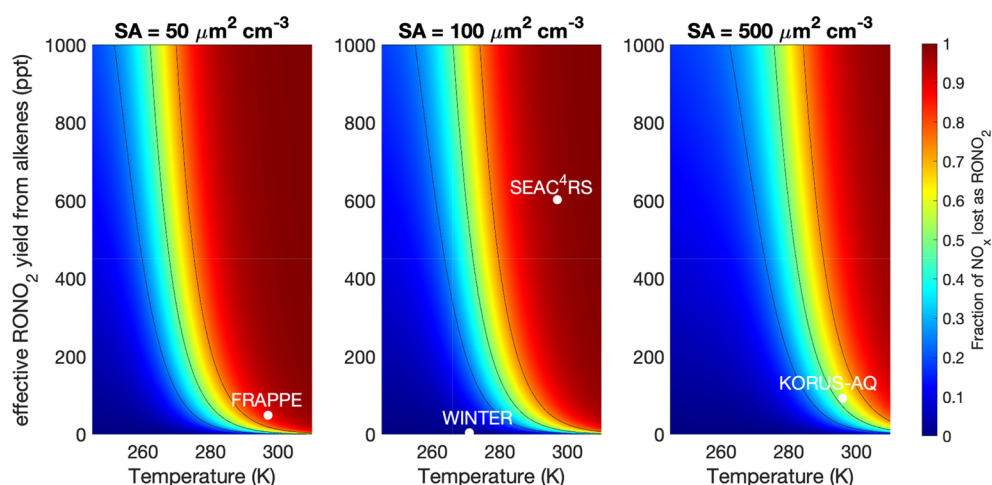


Figure 3. Fraction of NO_x lost as RONO_2 (defined as $\frac{P(\text{RONO}_2)}{P(\text{RONO}_2) + P(\text{HNO}_3)}$) overnight, shown as a function of temperature and effective RONO_2 yield from alkenes ($\sum_i \alpha_i [\text{alkene}]_i$) for three different aerosol surface areas ($\text{SA} = 50, 100, \text{ and } 500 \mu\text{m}^2 \text{cm}^{-3}$). We assume an initial NO_2 concentration (1 ppb), constant O_3 (40 ppb), constant pressure (1013 hPa), constant $\gamma(\text{N}_2\text{O}_5)$ (0.04), and NO_3 and N_2O_5 in steady state. Black contour lines correspond to 25%, 50%, and 75% of NO_x lost as RONO_2 . Average evening (after 16:30 local time) conditions during SEAC⁴RS, FRAPPE, and KORUS-AQ are shown. Average conditions during WINTER (NSF aircraft campaign over Northeastern United States during February to Mar 2015) are also shown as an example of conditions during which N_2O_5 loss is the dominant nighttime sink of NO_x (Kenagy et al., 2018).

N_2O_5 hydrolysis (Kenagy et al., 2018). Histograms of the distribution of the fraction of NO_x lost as RONO_2 calculated from evening observations of NO_2 , O_3 , alkenes, temperature, and pressure during each campaign can be found in Figures S7–S9.

Here we have presented evidence for a significant, and sometimes dominant, nighttime source of RONO_2 using airborne, daytime measurements. Further measurements of the diel cycles of RONO_2 and its precursors would be of use to further elucidate the relative importance of the different mechanisms for RONO_2 formation. Additionally, measurements of the diel cycle of RONO_2 could provide insights into the fate of daytime- and nighttime-produced RONO_2 by showing whether they remain in the gas phase or partition into particles and whether hydrolysis, oxidation, or deposition dominates loss of RONO_2 .

Appendix A: Calculating Fraction of NO_x Lost as RONO_2 Overnight

We calculate the nighttime production of RONO_2 from reaction of NO_3 and alkenes (R9) and the nighttime loss of N_2O_5 from heterogeneous hydrolysis (approximated as production of HNO_3) as

$$P(\text{RONO}_2) = \sum_i \alpha_i \times k_{\text{NO}_3 + \text{alkene}_i} \times [\text{alkene}_i] \times [\text{NO}_3] \quad (\text{A1})$$

$$P(\text{HNO}_3) = k_{\text{hyd}}[\text{N}_2\text{O}_5], \quad \text{where} \quad k_{\text{hyd}} = \frac{1}{4} \times \bar{c}_{\text{N}_2\text{O}_5} \times \text{SA} \times \gamma(\text{N}_2\text{O}_5). \quad (\text{A2})$$

Here α is the $\langle \text{INF} \rangle < I > i < / I > < / \text{INF} \rangle$ branching ratio for RONO_2 production from the reaction of NO_3 with alkenes, $\bar{c}_{\text{N}_2\text{O}_5}$ represents the mean molecular speed of N_2O_5 , $\gamma(\text{N}_2\text{O}_5)$ represents the heterogeneous uptake coefficient for N_2O_5 , and SA represents the aerosol surface area per volume of air.

We use the rate constant for the reaction of $\text{NO}_3 + \text{isoprene}$ for $k_{\text{NO}_3 + \text{alkene}}$. Values for $k_{\text{NO}_3 + \text{alkene}}$ and for k_b (defined below) are from the IUPAC chemical kinetics database (Atkinson et al., 2004, 2006). Values for $k_{\text{NO}_2 + \text{O}_3}$ and for k_f are from JPL Data Evaluation #18 (Burkholder et al., 2015). We assume an initial mixing ratio of NO_2 (1 ppb), and constant O_3 (40 ppb), pressure (1013 hPa), and $\gamma(\text{N}_2\text{O}_5)$ (0.04). Additionally, we assume NO_3 and N_2O_5 in steady state:

$$[\text{NO}_3]_{\text{SS}} = \frac{k_{\text{NO}_2 + \text{O}_3} [\text{NO}_2] [\text{O}_3]}{k_{\text{NO}_3 + \text{alkene}} [\text{alkene}]} \quad (\text{A3})$$

$$[\text{N}_2\text{O}_5]_{\text{SS}} = \frac{k_f[\text{NO}_3][\text{NO}_2]}{k_b + k_{\text{hyd}}}, \quad (\text{A4})$$

where k_f represents the formation of N_2O_5 from NO_2 and NO_3 and k_b represents the decomposition of N_2O_5 into NO_2 and NO_3 .

Acknowledgments

This work was supported by NASA grant 80NSSC18K0624 and an NSF Graduate Research Fellowship to H.S.K. (DGE1106400). This material is based upon work supported by the National Center for Atmospheric Research, which is a major facility sponsored by the National Science Foundation under Cooperative Agreement No. 1852977. We thank the science teams of SEAC⁴RS, FRAPPÉ, and KORUS-AQ. Data from SEAC⁴RS are available at <https://www-air.larc.nasa.gov/cgi-bin/ArcView/seac4rs>. Data from FRAPPÉ are available at https://data.eol.ucar.edu/master_lists/generated/frappe/. Data from KORUS-AQ are available at <https://www-air.larc.nasa.gov/cgi-bin/ArcView/korusaq?DC8=1>.

References

- Apel, E. C., Hornbrook, R. S., Hills, A. J., Blake, N. J., Barth, M. C., Weinheimer, A. J., et al. (2015). Upper tropospheric ozone production from lightning NO_x -impacted convection: Smoke ingestion case study from the DC3 campaign. *Journal of Geophysical Research: Atmosphere*, *120*, 2505–2523. <https://doi.org/10.1002/2014JD022121>
- Atkinson, R., Baulch, D. L., Cox, R. A., Crowley, J. N., Hampson, R. F., Hynes, R. G., et al. (2004). Evaluated kinetic and photochemical data for atmospheric chemistry: Volume I - gas phase reactions of O_x , HO_x , NO_x and SO_x species. *Atmospheric Chemistry and Physics*, *4*(6), 1461–1738. <https://doi.org/10.5194/acp-4-1461-2004>
- Atkinson, R., Baulch, D. L., Cox, R. A., Crowley, J. N., Hampson, R. F., Hynes, R. G., et al. IUPAC Subcommittee (2006). Evaluated kinetic and photochemical data for atmospheric chemistry: Volume II - gas phase reactions of organic species. *Atmospheric Chemistry and Physics*, *6*(11), 3625–4055. <https://doi.org/10.5194/acp-6-3625-2006>
- Ayres, B. R., Allen, H. M., Draper, D. C., Brown, S. S., Wild, R. J., Jimenez, J. L., et al. (2015). Organic nitrate aerosol formation via NO_3 + biogenic volatile organic compounds in the southeastern United States. *Atmospheric Chemistry and Physics*, *15*(23), 13,377–13,392. <https://doi.org/10.5194/acp-15-13377-2015>
- Brown, S. S., An, H., Lee, M., Park, J. H., Lee, S. D., Fibiger, D. L., et al. (2017). Cavity enhanced spectroscopy for measurement of nitrogen oxides in the Anthropocene: Results from the Seoul tower during MAPS 2015. *Faraday Discuss*, *200*, 529–557. <https://doi.org/10.1039/c7fd00001d>
- Brown, S. S., Dubé, W. P., Peischl, J., Ryerson, T. B., Atlas, E., Warneke, C., et al. (2011). Budgets for nocturnal VOC oxidation by nitrate radicals aloft during the 2006 Texas Air Quality Study. *Journal of Geophysical Research*, *116*, D24305. <https://doi.org/10.1029/2011JD016544>
- Burkholder, J. B., Sander, S. P., Abbatt, J. P. D., Barker, J. R., Huie, R. E., Kolb, C. E., et al. (2015). Chemical Kinetics and Photochemical Data for Use in Atmospheric Studies, Evaluation No. 18 (Tech. Rep.) Pasadena: Jet Propulsion Laboratory. <https://jpldataeval.jpl.nasa.gov>
- Colbeck, I., & Harrison, R. M. (1985). Dry deposition of ozone: Some measurements of deposition velocity and of vertical profiles to 100 metres. *Atmospheres Environment*, *19*(11), 1807–1818. [https://doi.org/10.1016/0004-6981\(85\)90007-1](https://doi.org/10.1016/0004-6981(85)90007-1)
- Colman, J. J., Swanson, A. L., Meinardi, S., Sive, B. C., Blake, D. R., & Rowland, F. S. (2001). Description of the analysis of a wide range of volatile organic compounds in whole air samples collected during PEM-Tropics A and B. *Analytical Chemistry*, *73*(15), 3723–3731. <https://doi.org/10.1021/ac010027g>
- Day, D. A., Dillon, M. B., Wooldridge, P. J., Thornton, J. A., Rosen, R. S., Wood, E. C., & Cohen, R. C. (2003). On alkyl nitrates, O_3 , and the missing NO_y . *Journal of Geophysical Research*, *108*(D16), JD003685. <https://doi.org/10.1029/2003JD003685>
- Day, D. A., Wooldridge, P. J., Dillon, M. B., Thornton, J. A., & Cohen, R. C. (2002). A thermal dissociation laser-induced fluorescence instrument for in situ detection of NO_2 , peroxy nitrates, alkyl nitrates, and HNO_3 . *Journal of Geophysical Research*, *107*(D6), 4046. <https://doi.org/10.1029/2001JD000779>
- Edwards, P. M., Aikin, K. C., Dubé, W. P., Fry, J. L., Gilman, J. B., De Gouw, J., et al. (2017). Transition from high- to low- NO_x control of night-time oxidation in the southeastern US. *Nature Geoscience*, *10*(7), 490–495. <https://doi.org/10.1038/ngeo2976>
- Fisher, J. A., Jacob, D. J., Travis, K. R., Kim, P. S., Marais, E. A., Chan, C., et al. (2016). Organic nitrate chemistry and its implications for nitrogen budgets in an isoprene- and monoterpene-rich atmosphere: Constraints from aircraft (SEAC⁴RS) and ground-based (SOAS) observations in the Southeast US. *Atmospheric Chemistry and Physics*, *16*, 5969–5991. <https://doi.org/10.5194/acp-16-5969-2016>
- Flocke, F., Pfister, G., Crawford, J. H., Pickering, K. E., Pierce, G., Bon, D., & Reddy, P. (2020). Air quality in the northern colorado front range metro area: The front range air pollution and photochemistry Experiment (FRAPPÉ). *Journal of Geophysical Research: Atmospheres*, *125*, e2019JD031197. <https://doi.org/10.1029/2019JD031197>
- Fry, J. L., Draper, D. C., Zarzana, K. J., Campuzano-Jost, P., Day, D. A., Jimenez, J. L., et al. (2013). Observations of gas- and aerosol-phase organic nitrates at BEACHON-RoMBAS 2011. *Atmospheric Chemistry and Physics*, *13*(17), 8585–8605. <https://doi.org/10.5194/acp-13-8585-2013>
- Horowitz, L. W., Fiore, A. M., Milly, G. P., Cohen, R. C., Perring, A., Wooldridge, P. J., et al. (2007). Observational constraints on the chemistry of isoprene nitrates over the eastern United States. *Journal of Geophysical Research*, *112*, D12S08. <https://doi.org/10.1029/2006JD007747>
- Huang, W., Saathoff, H., Shen, X., Ramisetty, R., Leisner, T., & Mohr, C. (2019). Chemical characterization of highly functionalized organonitrates contributing to night-time organic aerosol mass loadings and particle growth. *Environment Science Technology*, *53*(3), 1165–1174. <https://doi.org/10.1021/acs.est.8b05826>
- Kenagy, H. S., Sparks, T. L., Ebben, C. J., Wooldridge, P. J., Lopez-Hilfiker, F. D., Lee, B. H., et al. (2018). NO_x lifetime and NO_y partitioning during WINTER. *Journal of Geophysical Research: Atmospheres*, *123*, 9813–9827. <https://doi.org/10.1029/2018JD028736>
- Kiendler-Scharr, A., Mensah, A. A., Friese, E., Topping, D., Nemitz, E., Prevot, A. S. H., et al. (2016). Ubiquity of organic nitrates from nighttime chemistry in the European submicron aerosol. *Geophysical Research Letters*, *43*, 7735–7744. <https://doi.org/10.1002/2016GL069239>
- Lee, Alex K. Y., Adam, M. G., Liggio, J., Li, S.-M., Li, K., Willis, M. D., et al. (2019). A large contribution of anthropogenic organo-nitrates to secondary organic aerosol in the Alberta oil sands. *Atmospheric Chemistry and Physics*, *19*, 12,209–12,219. <https://doi.org/10.5194/acp-19-12209-2019>
- Lee, B. H., Mohr, C., Lopez-Hilfiker, F. D., Lutz, A., Hallquist, M., Lee, L., et al. (2016). Highly functionalized organic nitrates in the southeast United States: Contribution to secondary organic aerosol and reactive nitrogen budgets. *Proceedings of the National Academy of Science*, *113*(6), 1516–1521. <https://doi.org/10.1073/pnas.1508108113>
- Lenschow, D. H., Pearson, R., & Stankov, B. B. (1981). Estimating the ozone budget in the boundary layer by use of aircraft measurements of ozone eddy flux and mean concentration. *Journal of Geophysical Research*, *86*(8 C), 7291–7297. <https://doi.org/10.1029/jc086ic08p07291>
- Liebmann, J., Sobanski, N., Schuladen, J., Karu, E., Hellén, H., Hakola, H., et al. (2019). Alkyl nitrates in the boreal forest: Formation via the NO_3 , OH and O_3 induced oxidation of BVOCs and ambient lifetimes. *Atmospheric Chemistry and Physics*, *3*, 1–23. <https://doi.org/10.5194/acp-2019-463>

- Nault, B. A., Campuzano-jost, P., Day, D. A., Schroder, J. C., Anderson, B., Beyersdorf, A. J., et al. (2018). Secondary organic aerosol production from local emissions dominates the organic aerosol budget over Seoul, South Korea, during KORUS-AQ. *Atmospheric Chemistry and Physics*, *18*, 17,769–17,800. <https://doi.org/10.5194/acp-18-17769-2018>
- Perring, A. E., Pusede, S. E., & Cohen, R. C. (2013). An observational perspective on the atmospheric impacts of alkyl and multifunctional nitrates on ozone and secondary organic aerosol. *Chemical Reviews*, *113*(8), 5848–5870. <https://doi.org/10.1021/cr300520x>
- Pye, H. O. T., Luecken, D. J., Xu, L., Boyd, C. M., Ng, N. L., Baker, K. R., et al. (2015). Modeling the current and future roles of particulate organic nitrates in the Southeastern United States. *Environment Science Technology*, *49*(24), 14,195–14,203. <https://doi.org/10.1021/acs.est.5b03738>
- Ridley, B. A., Walega, J. G., Dye, J. E., & Grahek, F. E. (1994). Distributions of NO, NO_x, NO_y, and O₃ to 12 km altitude during the summer monsoon season over New Mexico. *Journal of Geophysical Research*, *99*(D12), 25,519–25,534. <https://doi.org/10.1029/94JD02210>
- Rollins, A. W., Browne, E. C., Min, K.-E., Pusede, S. E., Wooldridge, P. J., Gentner, D. R., et al. (2012). Evidence for NO_x control over nighttime SOA formation. *Science* (80-.), *337*(6099), 1210–1212. <https://doi.org/10.1126/science.1221520>
- Romer Present, P. S., Zare, A., & Cohen, R. C. (2020). The changing role of organic nitrates in the removal and transport of NO_x. *Atmospheric Chemistry and Physics*, *20*, 267–279. <https://doi.org/10.5194/acp-20-267-2020>
- Ryerson, T. B., Huey, L. G., Knapp, K., Neuman, J. A., Parrish, D. D., Sueper, D. T., & Fehsenfeld, F. C. (1999). Design and initial characterization of an inlet for gas-phase NO_y measurements from aircraft. *Journal of Geophysical Research*, *104*(D5), 5483–5492.
- Ryerson, T. B., Williams, E. J., & Fehsenfeld, F. C. (2000). An efficient photolysis system for fast-response NO₂ measurements. *Journal of Geophysical Research*, *105*(D21), 26,447–26,461. <https://doi.org/10.1029/2000JD900389>
- Simpson, I. J., Akagi, S. K., Barletta, B., Blake, N. J., Choi, Y., Diskin, G. S., et al. (2011). Boreal forest fire emissions in fresh Canadian smoke plumes: C₁ – C₁₀ volatile organic compounds (VOCs), CO₂, CO, NO₂, NO, HCN, and CH₃CH. *Atmospheric Chemistry and Physics*, *11*, 6445–6463. <https://doi.org/10.5194/acp-11-6445-2011>
- Sobanski, N., Thieser, J., Schuladen, J., Sauvage, C., Song, W., Williams, J., et al. (2017). Day- and night-time formation of organic nitrates at a forested mountain-site in South West Germany. *Atmospheric Chemistry and Physics*, *17*, 4115–4130. <https://doi.org/10.5194/acp-17-4115-2017>
- Starn, T. K., Shepson, P. B., Bertman, S. B., Riemer, D. D., Zika, R. G., & Olszyna, K. (1998). Nighttime isoprene chemistry at an urban-impacted forest site. *Journal of Geophysical Research*, *103*(D17), 22,437–22,447. <https://doi.org/10.1029/98JD01201>
- Toon, O. B., Maring, H., Dibb, J. E., Ferrare, R., Jacob, D. J., Jenson, E. J., et al. (2016). Planning, implementation, and scientific goals of the Studies of Emissions and Atmospheric Composition, Clouds and Climate Coupling by Regional Surveys (SEAC⁴RS) field mission. *Journal of Geophysical Research: Atmospheres*, *121*, 4967–5009. <https://doi.org/10.1002/2015JD024297>
- von Kuhlmann, R., Lawrence, M. G., Pöschl, U., & Crutzen, P. J. (2004). Sensitivities in global scale modeling of isoprene. *Atmospheric Chemistry and Physics*, *4*, 1–17. <https://doi.org/10.5194/acp-4-1-2004>
- Weinheimer, A. J., Walega, J. G., Ridley, B. A., Gary, B. L., Blake, D. R., Blake, N. J., et al. (1994). Meridional distributions of NO_x, NO_y, and other species in the lower stratosphere and upper troposphere during AASE II. *Geophysical Research Letters*, *21*(23), 2583–2586. <https://doi.org/10.1029/94GL01897>
- Wooldridge, P. J., Perring, A. E., Bertram, T. H., Flocke, F. M., Roberts, J. M., Singh, H. B., et al. (2010). Total peroxy nitrates (ΣPNs) in the atmosphere: The thermal dissociation-laser induced fluorescence (TD-LIF) technique and comparisons to speciated PAN measurements. *Atmosphere Measurement Technical*, *3*(3), 593–607. <https://doi.org/10.5194/amt-3-593-2010>
- Xiong, F., McAvey, K. M., Pratt, K. A., Groff, C. J., Hostetler, M. A., Lipton, M. A., et al. (2015). Observation of isoprene hydroxynitrates in the Southeastern United States and implications for the fate of NO_x. *Atmospheric Chemistry and Physics*, *15*, 11,257–11,272. <https://doi.org/10.5194/acp-15-11257-2015>
- Xu, L., Guo, H., Boyd, C. M., Klein, M., Bougiatioti, A., Cerully, K. M., et al. (2015). Effects of anthropogenic emissions on aerosol formation from isoprene and monoterpenes in the southeastern United States. *Proceedings of the National Academy of Science U. S. A.*, *112*(1), 37–42. <https://doi.org/10.1073/pnas.1417609112>
- Xu, L., Suresh, S., Guo, H., Weber, R. J., & Ng, N. L. (2015). Aerosol characterization over the southeastern United States using high-resolution aerosol mass spectrometry: Spatial and seasonal variation of aerosol composition and sources with a focus on organic nitrates. *Atmospheric Chemistry and Physics*, *15*(13), 7307–7336. <https://doi.org/10.5194/acp-15-7307-2015>